A MATLAB TOOL FOR VISUALIZING THE 3D POLAR POWER PATTERNS AND EXCITATIONS OF CONFORMAL ARRAYS

J. C. BRÉGAINS (MEMBER, IEEE), J. A. GARCÍA-NAYA (MEMBER, IEEE),

A. DAPENA (MEMBER, IEEE), AND M. GONZÁLEZ-LÓPEZ (MEMBER, IEEE)

Electronic Technology and Communications Group, Department of Electronics and Systems, 15701 Campus Elviña, University of A Coruña (Spain)

e-mails: (Brégains) julio.bregains@udc.es – (García-Naya) jagarcia@udc.es

(Dapena) adriana@udc.es – (González-López) mgonzalezlopez@udc.es

ABSTRACT

This paper describes the implementation of a MATLAB® tool to plot the 3D polar radiation diagram generated by a conformal antenna array. A related tool has also been developed for visualizing the geometrical arrangement (positions and orientations) of the elements, as well as the relative values of the amplitude and phase of their excitations. Supporting M-files are available.

1. INTRODUCTION

Currently, there is a broad set of computer tools available for any antenna designer for manipulating equations, numerical algorithms and/or plotting two–dimensional (2D) or three–dimensional (3D) functions. In this sense, there is no doubt that, lately, MATLAB® [1-2] reigns supreme as the most widely used numerical computing environment for performing calculations applied to technical sciences and engineering. This is not surprising, because with a minimum knowledge about basic MATLAB® functions, it is possible not only to manipulate data and carry out accurate computations in a fast and simple way, but also to create very instructive graphics in little time.

In an earlier work [3], a MATLAB® tool to plot both the power pattern and the excitation (amplitude and phase) distribution of a planar array antenna was presented. That tool had the drawback of not being designed to represent power patterns generated by conformal arrays (namely, an array whose geometry is adapted to a previously established surface, not necessarily flat [4]). Such a drawback was a consequence of not taking into account elements having a 3D spatial distribution with rotations associated to them. Based upon the source code described in that work, here we present a tool capable of representing the polar power pattern radiated by conformal antenna arrays as well as its geometrical and electrical configurations.

2. THE METHOD

Here we first describe mathematically the problem and then describe the proposed tool to solve it.

2.1. Mathematical Description: Radiation Emitted by a Conformal Array

Suppose we have a set of *N* antennas in a bounded space, see Figure 1. For simplicity, consider all of them having the same geometrical and electrical configuration, in such a way that, if any of them were located on the center of a global coordinates system (*x*,*y*,*z*), it would radiate, at a very distant point *P* specified by the position vector **R**, a complex–valued field $f_e(\theta,\varphi)$. As each element *n* is not only displaced from the center to a certain position $\mathbf{r}_n$, but also correspondingly rotated so as to keep associated to it a local coordinates system (x_n,y_n,z_n), the field at point *P* becomes:

$$f_e\ \theta_n,\varphi_n\ e^{j\mathbf{k}\cdot\mathbf{r}_n} \tag{1}$$

where $\mathbf{k} = (2\pi/\lambda)\mathbf{a}_R$ is the wave vector [5], with λ representing the wavelength at the working frequency of the array, and $\mathbf{a}_R$ the unitary vector pointing radially towards *P*. As it can be seen from Figure 1, now the (θ,φ) angles are measured from the local coordinates system, thus becoming (θ_n,φ_n). It can be observed also that, being *P* a point located at far field [5], **R** and $\mathbf{R}_n$ (that are virtually pointing to the infinity) can be considered to be parallel vectors.

The complex field radiated by the whole array is then obtained after applying the superposition principle (and neglecting, for simplicity, the electromagnetic coupling between contiguous elements):

$$F\ \theta,\varphi\ = \sum_{n=1}^{N} f_e\ \theta_n,\varphi_n\ I_n e^{j\mathbf{k}\cdot\mathbf{r}_n} \tag{2}$$

The (complex–valued) phasors $I_n = |I_n|e^{j\Phi n}$ specify the amplitude factor $|I_n|$ and relative phase Φ_n applied to the *n*–th element's signal. As usual, *F* can be measured in dB: $|F(\theta,\varphi)|_{dB} = 10\log_{10}|F|^2$, with $|F|^2$ representing the (averaged over time) power density (W/m^2).

The greatest difficulty for calculating Equation (2) numerically lies on the proper computation of the (θ_n,φ_n) angles, which requires obtaining the local coordinate system associated to each element. To this end, the traditional approach consists in establishing, for each element, three consecutive rotations until the proper position is reached. Those rotations are specified by the well known Euler angles [6], which make possible the implementation of appropriate coordinate transformations through matrix multiplications. As an intuitive alternative, we propose to avoid such transformations in the implementation, instead using directly, as inputs, the direction angles belonging to each axis of the local coordinates system associated to each element. For example, the x_n axis has associated with it three angles $\alpha_{xn},\beta_{xn},\gamma_{xn}$, measured with respect to *x*, *y* and *z* axes, respectively; in the same way, $\alpha_{yn},\beta_{yn},\gamma_{yn}$ angles are related to y_n axis. Each set of (six) angles allows the calculation of the corresponding direction cosines and, consequently, the linked unitary vectors. Once the unitary

vectors of those axes are obtained, it is possible to further calculate the unitary vector of z_n by means of cross vector multiplication. Next, once the x_n,y_n and z_n axes are calculated, the angles θ_n and φ_n are obtained with the following expressions (see Figure 1):

$$\theta_n = \text{acos}\left(\mathbf{a}_R \cdot \mathbf{a}_{zn}\right);\ \varphi_n = \text{atan}\left(\frac{a_{\rho y_n}}{a_{\rho x_n}}\right) \tag{3}$$

$$\text{with } \mathbf{a}_{\rho n} = \frac{\mathbf{a}_R - \mathbf{a}_{Zn}\cos\theta_n}{sen\,\theta_n} = a_{\rho nx}\mathbf{a}_x + a_{\rho ny}\mathbf{a}_y + a_{\rho nz}\mathbf{a}_z = a_{\rho nx_n}\mathbf{a}_{xn} + a_{\rho ny_n}\mathbf{a}_{yn} + a_{\rho nz_n}\mathbf{a}_{zn} \tag{4}$$

being the components

$$\begin{aligned} a_{\rho nx_n} &= a_{\rho nx}x_{xn} + a_{\rho ny}y_{xn} + a_{\rho nz}z_{xn} \\ a_{\rho ny_n} &= a_{\rho nx}x_{yn} + a_{\rho ny}y_{yn} + a_{\rho nz}z_{yn} \\ a_{\rho nz_n} &= a_{\rho nx}x_{zn} + a_{\rho ny}y_{zn} + a_{\rho nz}z_{zn} \end{aligned} \tag{5}$$

obtained after considering the direct and inverse transformations **T** and $\mathbf{T}^{-1}$, respectively; namely:

$$\begin{bmatrix}\mathbf{a}_{xn}\\ \mathbf{a}_{yn}\\ \mathbf{a}_{zn}\end{bmatrix} = \begin{bmatrix}x_{nx} & x_{ny} & x_{nz}\\ y_{nx} & y_{ny} & y_{nz}\\ z_{nx} & z_{ny} & z_{nz}\end{bmatrix}\begin{bmatrix}\mathbf{a}_x\\ \mathbf{a}_y\\ \mathbf{a}_z\end{bmatrix} \Rightarrow \mathbf{a}_n = \mathbf{T}\mathbf{a};\ \begin{bmatrix}\mathbf{a}_x\\ \mathbf{a}_y\\ \mathbf{a}_z\end{bmatrix} = \begin{bmatrix}x_{xn} & x_{yn} & x_{zn}\\ y_{xn} & y_{yn} & y_{zn}\\ z_{xn} & z_{yn} & z_{zn}\end{bmatrix}\begin{bmatrix}\mathbf{a}_{xn}\\ \mathbf{a}_{yn}\\ \mathbf{a}_{zn}\end{bmatrix} \Rightarrow \mathbf{a} = \mathbf{T}^{-1}\mathbf{a}_n\ ; \tag{6}$$

It is important to note that the use of expression on the right-hand side of Equation (3) instead of the simpler[1] φ_n = acos($\mathbf{a}_{\rho n}\cdot\mathbf{a}_{xn}$) was justified by the fact that φ_n is ranged from 0 to 2π, a condition that is fulfilled by using the atan2() function –a proper MATLAB® adaptation of atan()– instead of acos().

2.2. The MATLAB® tool.

From now on we describe briefly the application which has been addressed.

The tool is started by invoking it in the MATLAB® command line. During the loading process, two input files are read. The first one contains the $\mathbf{r}_n = (\xi_n, \psi_n, \zeta_n)$ vector components –measured in units of λ – of the position of each of the *N* elements, followed by the amplitude $|I_n|$ and phase Φ_n (measured in degrees, between 0º and 360º) of their complex excitations I_n. Consequently, the input file will have those values arranged in five columns and *N r*ows. The second file contains the direction angles of the local axes x_n and y_n of each element, thus being arranged in six columns and *N* rows.

After reading those files and storing the data into the computer memory, the program calculates, with the aid of the direction angles, the unitary vectors $\mathbf{a}_{xn}$ and $\mathbf{a}_{yn}$ (see Figure 1). Next, the program proceeds to obtain, by utilizing the cross product, the remaining unitary vectors $\mathbf{a}_{zn}$.

[1] The dot product $\mathbf{a}_{\rho n}\cdot\mathbf{a}_{xn}$ would not need any inverse transform $\mathbf{T}^{-1}$ previously calculated, see equations (6).

In a further step, the program asks the user for the spatial distribution of the elements to be plotted or not. If the plot is requested, then the conformal array is shown as a set of circles, each one representing an element of the array. The program determines automatically the maximum size of the array (in λ units) in order to plot a set of Cartesian axes whose proportions fit the ones of the array. The program can also handle the one–element case (located at the center of the coordinate system), which allows the user to study the $f_e(\theta,\varphi)$ function of a single antenna.

Afterwards, the program asks for the excitation amplitude distribution to be plotted. If requested, a corresponding plot shows, for each element of the array, a cone whose axis of revolution coincides with the z_n axis of such an element, and whose height is proportional to the corresponding excitation normalized amplitude (i.e., the program normalizes the amplitudes, making $0 \leq |I_n| \leq 1$, $\forall n \in [1,N]$). The constant factor of proportionality A_f applied to the height will be a value to be specified by the user in the code; in this way, $A_f = 1$, for example, indicates that, when the oriented amplitude distribution is represented, the cones are measured in wavelength units, and their heights vary between 0 (for $|I_n| = 0$) and λ (for $|I_n| = 1$). In the same way, R_f corresponds to a factor for the radius of the cones. In order to represent the conical surfaces, it is necessary to use parametric equations. It is important to note that these parametric equations must be established in global coordinates. Under this assumption, by considering the direct transformation given by the left-hand side of Equation (6), we arrive to the following expression for the parametric representation of the n–th cone:

$$\begin{aligned}\mathbf{C}_n = &\left\{R_f(1-t)\left[\cos(2\pi t)x_{nx} + \operatorname{sen}(2\pi t)y_{nx}\right] + A_f|I_n|tz_{nx} + \xi_n\right\}\mathbf{a}_x + \\ &+\left\{R_f(1-t)\left[\cos(2\pi t)x_{ny} + \operatorname{sen}(2\pi t)y_{ny}\right] + A_f|I_n|tz_{ny} + \psi_n\right\}\mathbf{a}_y + \\ &+\left\{R_f(1-t)\left[\cos(2\pi t)x_{nz} + \operatorname{sen}(2\pi t)y_{nz}\right] + A_f|I_n|tz_{nz} + \zeta_n\right\}\mathbf{a}_z\end{aligned} \quad (7)$$

with the parameter t ranging from 0 to 1.

Equation (7) can be handled more efficiently in MATLAB® by considering matrix operations, as observed in the portion of the source code shown below, where the meaning of each variable is easily deduced from its name:

```
hold on;                                % Allow drawing the cones in the active window
t = 0:1/14:1;                           % Parametric variable vector t
th=2*pi*t;                              % Parametric angle
costh=cos(th); sinth=sin(th);           % cos(2*pi*t) and sin(2*pi*t) components
rcone=Rf*(1-t);                         % Variable radius of cones
ident=ones(1, size(t,2));               % Identity vector (same size as vector t)
rident=Rf*ident;                        % Constant radius of the base of the cones
 for(n=1:N)                             % For each element, build up the parametric matrices
        Xpc=rcone'*(costh*Xn(n,1)+sinth*Yn(n,1))+Af*AmpIn(n,1)*t'*ident*Zn(n,1)+rn(n,1);
```

```
            Ypc=rcone'*(costh*Xn(n,2)+sinth*Yn(n,2))+Af*AmpIn(n,1)*t'*ident*Zn(n,2)+rn(n,2);
            Zpc=rcone'*(costh*Xn(n,3)+sinth*Yn(n,3))+Af*AmpIn(n,1)*t'*ident*Zn(n,3)+rn(n,3);
           %  Now plot the n-th cone by using Xpc, Ypc and Zpc matrices…
               ps=surf(Xpc,Ypc,Zpc,'EdgeColor', 'red', 'EdgeAlpha', 0.40, 'LineWidth', 0.50);
           % Set the cone color to red, and apply certain degree of transparency …
               set(ps,'FaceColor',[1.000 0.502 0.502]); alpha(0.75);
    end;
    hold off;                                   % The control over the active window is no longer necessary
```

Once the amplitude oriented cones are represented, the program asks the user to specify whether the phase distribution is plotted or not, this time by means of vertical (non–oriented) cones. In such a case, the relative phases are specified by heights ranging from zero (Φ_n=0º) to λ (Φ_n=360º), conveniently resized by a proportionality factor P_f.

Finally, the program gives the option of plotting the 3D polar radiation diagram, whether over the upper spatial hemisphere ($0 \le \theta \le 90º$, $0 \le \varphi \le 360º$) or the whole space ($0 \le \theta \le 180º$, $0 \le \varphi \le 360º$). The normalized radiation pattern is now represented by means of a parametrized polar surface. The radial coordinate of such a surface, being a function of the θ and φ parameters, indicates the power density value, expressed in dB. The procedure for plotting the power pattern is derived from the source code described in [3], but considering a convenient adaptation to Equation (2), and using the transformations given in Equations (3) to (6). The interested reader is referred to [3] for more information about the abovementioned source code.

3. EXAMPLES

This section is devoted to present several examples in order to show the scope as well as the limitations of the implementation.

3.1. Half–wavelength Dipole Subject to Several Rotations

As a first example, we consider the radiation diagram of a single $\lambda/2$ dipole aligned along the *y* axis, centered on the origin of the coordinates system, and backed by an infinite groundplane parallel to the $z = 0$ plane (and located at $z = -0{,}25\lambda$). This first example just serves to verify the appropriate rotation of the radiation diagram, according to the rotation applied to the dipole itself. The far field element factor $f_e(\theta,\varphi)$ used in this case is the one specified in [7], conveniently adapted (null radiation below the ground plane).

Figure 2 shows the obtained patterns. The first one (top left) corresponds to a radiation diagram attained when the dipole lies along the *y* axis. In this case, the local axes of the dipole match the global ones: $x_1 = x$, $y_1 = y$, $z_1 = z$, or, which is the same, $\alpha_{x1} = 0º$, $\beta_{x1} = 90º$, $\gamma_{x1} = 90º$, $\alpha_{y1} = 90º$, $\beta_{y1} = 0º$,

γ_{y1} = 90º. The second graphic (top right) represents the pattern after rotating the dipole (and the ground plane) 45º degrees about the *z* axis, i.e., α_{x1} = 45º, β_{x1} = 45º, γ_{x1} = 90º, α_{y1} = 135º, β_{y1} = 45º, γ_{y1} = 90º. The bottom left graph is obtained by rotating the ground plane 45º about the *y* axis (it is not necessary to rotate the dipole): α_{x1} = 45º, β_{x1} = 90º, γ_{x1} = 135º, α_{y1} = 90º, β_{y1} = 0º, γ_{y1} = 90º. Finally, the bottom right figure shows the pattern after rotating the dipole 30º about the *x* axis.

In all graphics, the acronym NPD [dB] stands for Normalized Power Density (expressed in decibels). For the sake of brevity, the single oriented cones are not represented in this example.

3.2. Semi-cylindrical array of dipoles with groundplanes

We depart from the expression of the element factor $f_e(\theta,\varphi)$ of a λ/2 dipole aligned along the z axis, with a groundplane parallel to the x = 0 plane and located a distance 0.25λ from the dipole [7]. In this way, 50 dipoles are conformed onto a semi-cylindrical surface with base radius equal to 2λ and a total height of 3.3λ (measured from the extremes of the top and bottom dipoles), so as the main axes of the dipoles z_n are tangential to the cylinder. The dipoles are arranged in 5 rows, the vertical separation between contiguous dipoles being 0.7λ, with each row containing 10 dipoles uniformly distributed along their corresponding semi-circles. The groundplane of each dipole is also tangential to the semi–cylindrical surface. The excitations of the dipoles are the result of multiplying (i.e. by using separable distributions [7]) those of a two linear arrays with triangular excitations (I_{nHoriz} = {1,2,3,4,5,5,4,3,2,1} and I_{mVert} = {1,2,3,2,1}). Figure 3 shows the spatial distribution of the dipoles, represented, as mentioned above, by circles. Figure 4 shows the amplitude excitation distribution, with the cones oriented along the axis of each dipole.

As Φ_n = 0º for all the elements, it is not necessary to represent the phase distribution. The power density pattern generated by this conformal array is shown in Figure 5.

3.3. Conical Array of Circular Patches

In this example we consider an element factor $f_e(\theta,\varphi) = \cos^2\theta$, which corresponds to the theoretical simple model of a circular patch (radiating only in the upper hemisphere). On the same conical surface used in the previous example forty patches are conformed, with the same distribution given for the dipoles, but oriented in such a way that the normal to each patch is also normal to the conical surface. The excitation distribution is as follows: the sixteen patches located at the edge of the base (first row) are fed with $I_n = e^{j135º}$, the twelve patches of the second row are uniformly excited with $I_n = 0{,}75e^{j90º}$; the eight patches of the following row have $I_n = 0{,}75e^{j45º}$, whereas, for the four ones of the last row, $I_n = 0{,}25e^{j0º}$. Figures 6 and 7 show the oriented amplitude and non–oriented phase distributions, respectively. Figure 6 was drawn by considering that each cone indicates a normal to the corresponding patch. Finally, the pattern radiated by this configuration is given in Figure 8.

4. CLOSING COMMENTS

The tool presented is useful for analyzing not only the geometrical configuration, but the electrical behaviour of conformal arrays, as well as the power patterns radiated by them. This is not only recommended as a diagnosis tool for antenna designers, but as an excellent complement for any educator whose lectures include the essentials of conformal arrays.

It is important to remark that the program was codified by bearing in mind the fundamental pedagogical use of the tool; therefore, it has not been optimized in terms of either code length or computing time.

The source code is freely available at http://gtec.des.udc.es/web/images/files/conformalpow3d.zip.

5. ACKNOWLEDGEMENTS

This work has been partially supported by: Xunta de Galicia, Ministry of Science and Innovation, and FEDER funds from the European Union (projects 09TIC008105PR, TEC2007–68020–C04–01, CSD2008–00010).

6. REFERENCES

[1]. The MATLAB Group, Inc.: “MATLAB Function Reference: Volumes 1-2-3”, PDF document (printable version taken from Help menu in MATLAB®), 2008.

[2]. The MATLAB Group, Inc., “MATLAB: 3-D Visualization,” PDF document (printable version taken from Help menu in MATLAB®), 2008.

[3]. J. C. Brégains, F. Ares, E. Moreno, "Visualizing the 3D Polar Power Patterns and Excitations of Planar Arrays with MATLAB," *IEEE Antennas and Propagation Magazine*, **46**, 2, 2004, pp. 108–112.

[4]. L. Josefsson, P. Persson, *Conformal Array Antenna Theory and Design*, IEEE Press, John Wiley & Sons, 2006.

[5]. C. A. Balanis, *Antenna Theory. Analysis and Design, Third Edition*, Wiley Interscience, 2005.

[6]. T. Milligan, “More Applications of Euler Rotation Angles”, *IEEE Antennas and Propagation Magazine*, **41**, 4, 1999, pp. 78–83.

[7]. R. S. Elliott, *Antenna Theory and Design*, *Revised Edition*, Wiley Interscience, 2003.

LEGENDS FOR FIGURES

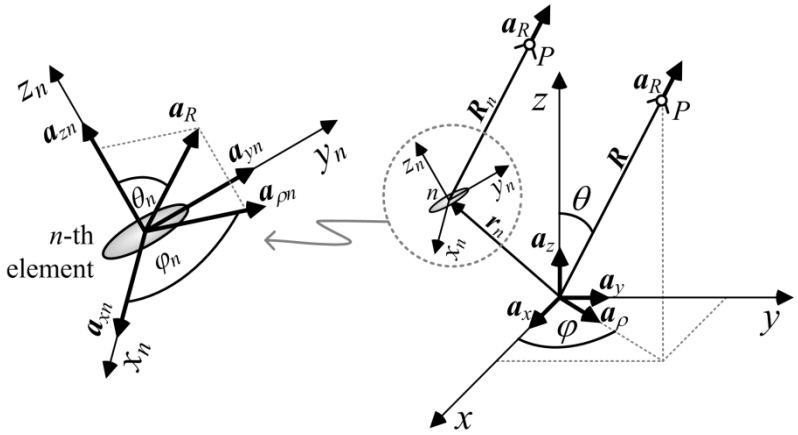

Figure 1. A set of elements of a conformal array in a bounded space, considering a global Cartesian coordinates system (x,y,z). Element n is characterized by its local coordinates (x_n,y_n,z_n, at the left–hand side), which are required to calculate the field radiated at a distant point P.

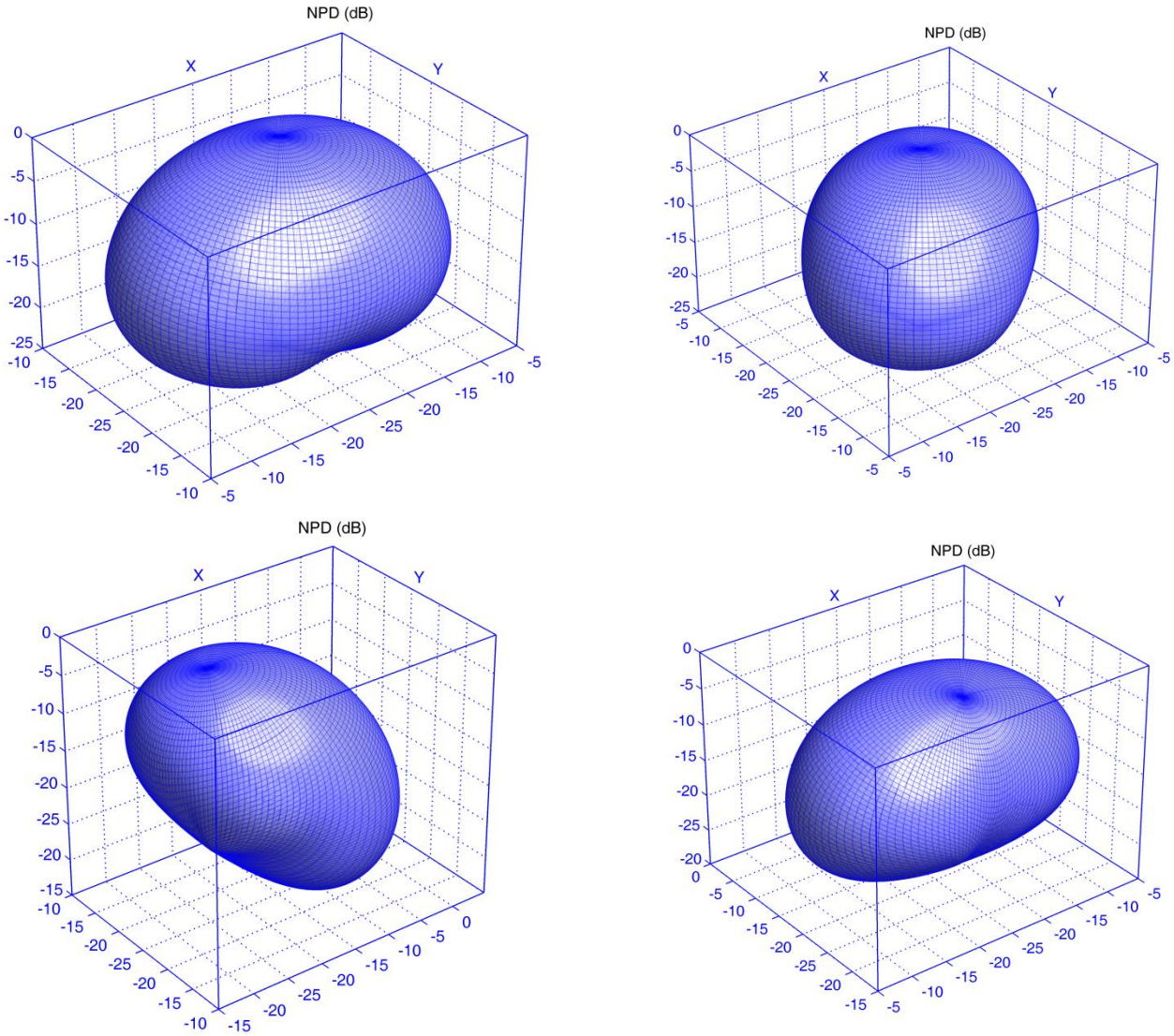

Figure 2. Power patterns radiated by a λ/2 dipole, backed by a groundplane located a distance –λ/4 away. Top left: pattern for dipole aligned along y axis. Top right: for dipole rotated 45º with respect to the z axis. Bottom left: pattern when the groundplane rotates –45º with respect to the y axis. Bottom right: for dipole rotated –30º with respect to the x axis.

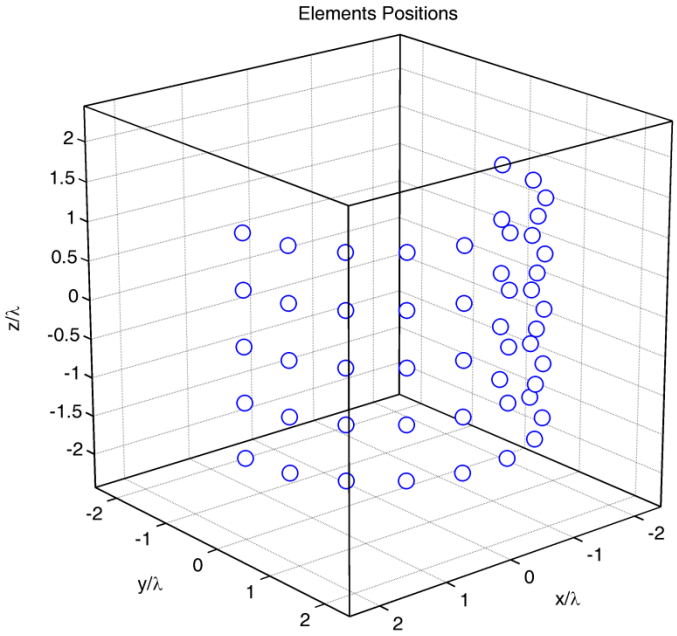

Figure 3. Arrangement of 50 dipoles on a semi-cylinder with base radius equal to 2λ and height equal to 3.3λ (see text). The vertical separation between contiguous dipoles is of 0.7λ. Each circle represents a dipole.

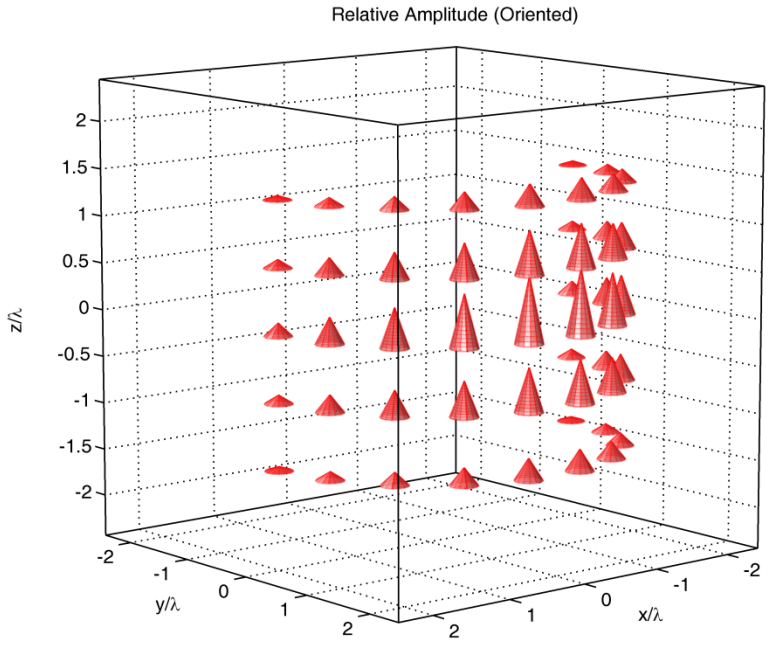

Figure 4. Amplitude distribution of the dipoles conformed on the semi-cylinder given in Figure 3. The lengths of the cones indicate the relative excitation amplitudes (see text), and their main axes coincide with the ones of the corresponding dipoles.

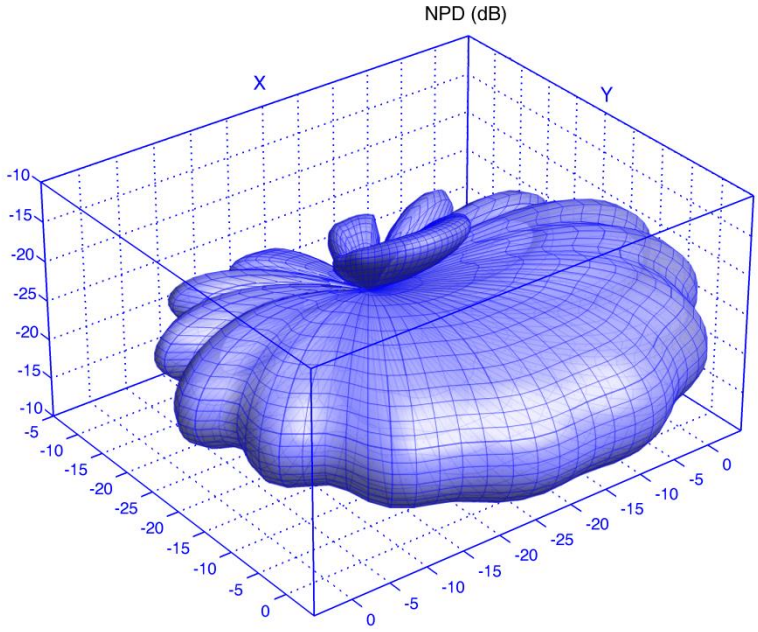

Figure 5. 3D polar plot of the power pattern of a conformal array of 50 dipoles with ground planes, arranged over a semi-cylinder, see Figure 4.

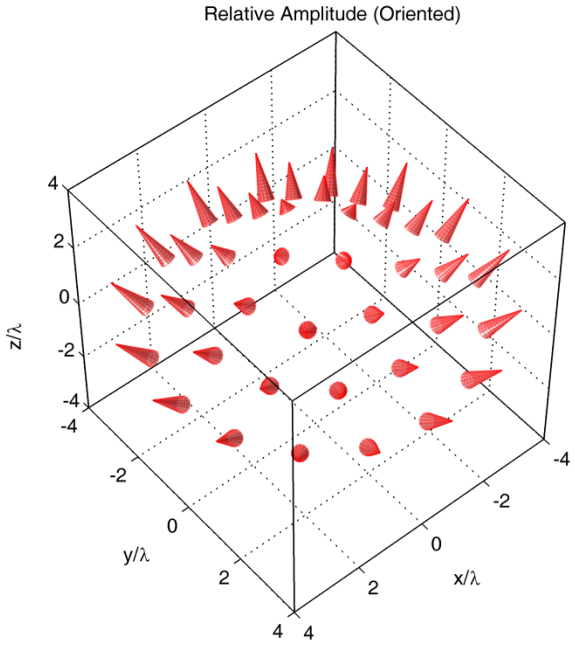

Figure 6. Amplitude distribution of 40 patches conformed over the surface given in Figure 3. The length of each cone indicates the excitation relative amplitude of each patch (see text), and the main axis of each one coincides with the normal to the corresponding patch.

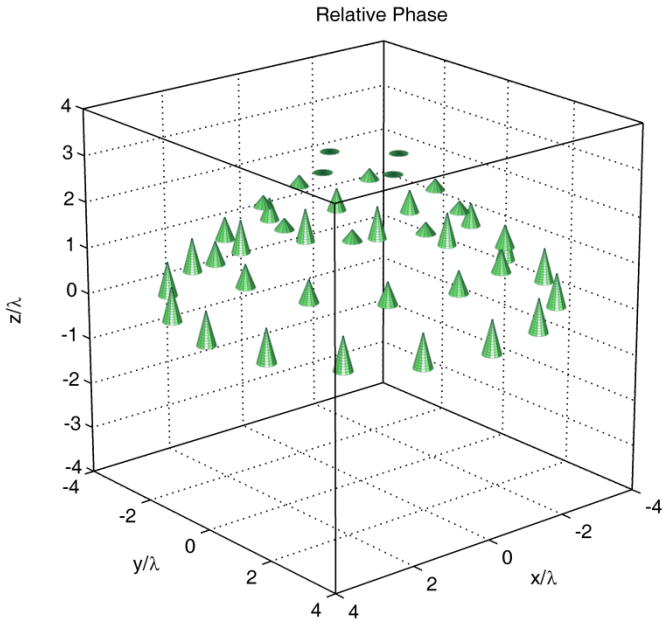

Figure 7. Relative phase distribution (given by the lengths of the little cones) of the patches conformed over a conical surface, see text.

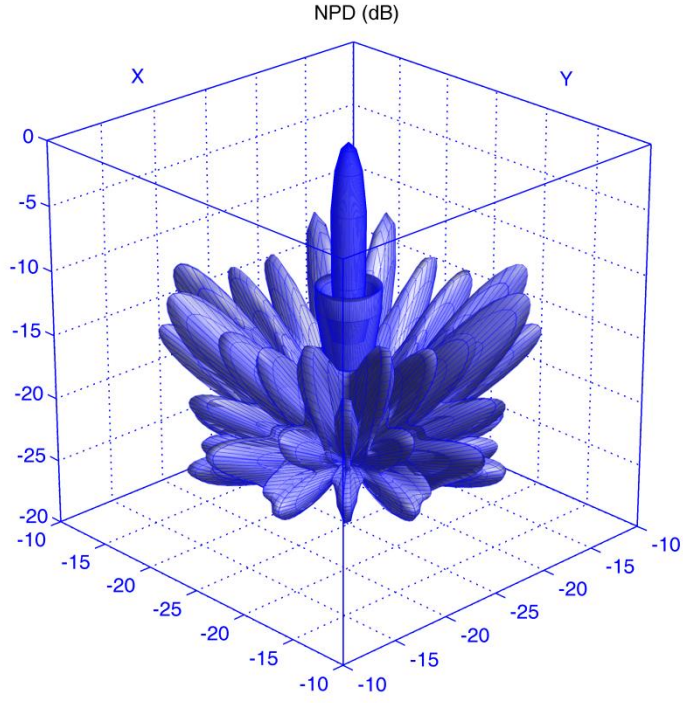

Figure 8. 3D polar plot of the power pattern of a conformal array of 40 patches arranged on a cone, see Figures 6 and 7.